

## BL Lacertae: Hard Optical Spectrum and GeV $\gamma$ -ray Emission

Shan-Jie Qian<sup>1</sup>, Xi-Zhen Zhang<sup>1</sup> and T. P. Krichbaum<sup>2</sup>

<sup>1</sup> National Astronomical Observatories, Chinese Academy of Sciences, Beijing 100012; rqsj@bao.ac.cn

<sup>2</sup> Max-Planck-Institut für Radioastronomie, Auf dem Hügel 69, 53121 Bonn, Germany

Received 2003 September 26; accepted 2004 March 4

**Abstract** The spectral energy distribution (SED) of the  $\gamma$ -ray flare observed in July 1997 in BL Lacertae is re-considered. It is pointed out that the optical observations made by Webb et al. showed the associated optical flare has a hard spectrum (the average spectral index  $\alpha_{\text{opt}} \sim 0.48$ ,  $F_{\nu} \propto \nu^{-\alpha}$ ), and the ASCA observations made by Tanihata et al. showed very steep spectra in the soft X-ray band (0.7–1.5 keV) ( $\alpha_x \sim 3 - 4$ ). We find that the flux densities and spectral indices in both the optical and soft X-ray bands are closely consistent with a ‘canonical’ synchrotron spectrum emitted by relativistic electrons of a power-law energy distribution with a high energy cutoff, and thus the peak of the SED of the synchrotron radiation (in representation of  $\nu F_{\nu}$ ) is located in the EUV – soft X-ray bands. Therefore, the GeV  $\gamma$ -ray emission observed in the July 1997 outburst may be mainly due to the synchrotron self-Compton (SSC) process, contrasting with the current explanations in terms of external radiation Compton (ERC) process, in which the seed photons are mostly taken to be the UV emission from the clouds of the broad emission line region. We argue that the hard optical spectra observed during the  $\gamma$ -ray outburst may be an important signature for the acceleration of high energy electrons ( $\gamma_e \sim 10^4$ ) in the  $\gamma$ -ray emitting region.

**Key words:** galaxies: compact – gamma rays: observations – quasars: individual: BL Lacertae

### 1 INTRODUCTION

The strong and variable emission from radio through  $\gamma$ -rays observed in blazars is nonthermal radiation emitted by relativistic jets pointing close to the line of sight. Simultaneous multi-wavelength observations (mainly at IR–optical through  $\gamma$ -ray wavelengths) have been made in recent years for some bright blazars to investigate their emission mechanism. Analyses of these observations have shown that the spectral energy distribution (SED) of blazars, as represented in the  $\nu$ – $\nu S_{\nu}$  plot, comprises two broad bumps: one in the radio to optical – UV– soft X-ray

region (in some cases even reaching hard X-ray bands); and the other in the X-ray to  $\gamma$ -ray region. The X-ray band is usually located at the cross of the two bumps, as a wide trough. From the high polarization of the radio to optical emission, the lower energy bump is shown to be due to synchrotron radiation by the relativistic electrons in the jet. The higher energy bump is believed to be produced via Compton up-scattering by the same population of relativistic electrons. Two main possibilities have been suggested for the source of the seed photons : (1) they can be the synchrotron photons within the emitting region itself (SSC models); and (2) they are external photons such as from the broad emission-line clouds or from the accretion disk (ERC models).

According to the characteristic properties of the objects and their SEDs, blazars are divided into the following three subclasses (Ulrich et al. 1997; Kubo et al. 1998; Ghisellini et al. 1998; Fossati et al. 1998; Sambruna et al. 1996; Padovani et al. 2001):

- (1) Flat spectrum radio quasars (FSRQs), with the peak frequency of the synchrotron component located in the IR–optical region and the luminosity dominated by the high-energy ( $\gamma$ -ray) component;
- (2) High-energy peaked BL Lac objects (HBLs, mostly X-ray selected BL Lac objects), with the peak of the synchrotron component normally located in UV–soft-X-ray region and the high and low energy components having similar luminosities;
- (3) Low-energy peaked BL Lac objects (LBLs, mostly radio selected BL Lac objects) with luminosities and synchrotron peak frequencies intermediate between the above two subclasses.

A remarkable feature of the relationship between the two components is that the peak frequency of both shifts toward higher energies (frequencies) when the source flares. HBLs, especially TeV blazars, show this trend most prominently. For example, in the XBL object Mrk 501 the synchrotron peak frequency was observed to be located at  $\sim 100$  keV in the 1997 April flares and the high energy component was observed to have TeV emission (Pian et al. 1998).

As is well known, FSRQs emit strong broad emission lines. Theoretical analyses of their SEDs and flaring activity have shown that external seed photons may play an important role in the production of their GeV  $\gamma$ -ray emission (e.g., Ghisellini et al. 1998; Madejski et al. 1999; Mukherjee et al. 1999). In contrast, BL Lac objects (both HBLs and LBLs) usually lack or have only very weak emission lines and thus it is thought that their  $\gamma$ -rays may be most likely due to the synchrotron self-Compton process.

As one of the best-studied blazars in radio to optical region, BL Lacertae is originally regarded as the prototype object for the BL Lac class. Based on its SED properties it may be classified as an LBL object. Its host galaxy is a giant elliptical at a redshift of 0.069 (Miller 1978). For a long time after its identification BL Lacertae was thought to have no broad emission lines. However, broad optical emission lines ( $H\alpha$  etc.) have recently been detected when the source was in a low-activity state, showing the existence of a broad emission line region (Vermeulen et al. 1995; Corbett et al. 1996; 2000). The detection of broad emission lines in BL Lacertae and other BL Lac objects reveals the similarity in nuclear structure between quasars and BL Lacs. Moreover, Corbett et al. (2000) showed that the equivalent width of the  $H\alpha$  line is anti-correlated with the intensity of the nonthermal jet emission and that the ionizing continuum may be due to the accretion disk. An important topic related to this detection is

whether the photons from the broad line emitting clouds could play a significant role (as seed photons in Compton process, e.g. Peterson 1997) in the production of  $\gamma$ -ray emission.

From BL Lacertae  $\gamma$ -ray emission was detected above  $>100$  MeV in two multiwavelength monitoring campaigns in 1995 July and 1997 July. The first detection was when the source was at a low-activity state and the second, a high-activity state, when a  $\gamma$ -ray flare was detected. Interpretations on the SED of the second event of 1997 July have been investigated by several authors. Model-fittings to the observed SED were made and it has been suggested that the strong GeV  $\gamma$ -ray emission detected in 1997 is due to the Compton up-scattering of external seed photons from its broad line emitting clouds (e.g., Böttcher et al. 2000, 2002; Madejski et al. 1999), because it was found that seed photons from the emitting region itself are not strong enough for producing GeV  $\gamma$ -rays through the SSC process.

Makino (1999) has suggested that the wideband MeV–GeV  $\gamma$ -ray flare observed in 1997 July could not be explained in terms of a homogeneous, one-component model, and multi-component or inhomogeneous models are required.

For the 1997 July  $\gamma$ -ray outburst Madejski et al. (1999) argued in favor of EC-models because of the lack of the seed photons from the synchrotron radiation itself. In their estimates for the seed photons they assumed that the synchrotron peak was located at  $\sim 2.4 \times 10^{14}$  Hz (1 eV, near *IR*-band) with a steep optical spectrum. Based on an SSC model they obtained that the bulk-motion Lorentz factor was required to be  $\Gamma \geq 100$  and the magnetic field, extremely weak ( $\sim 10^{-4}$  G). Madejski et al. (1999) suggested that the EGRET detection of GeV radiation from BL Lacertae is connected with the emergence of optical broad emission lines. They argued that in 1992 and 1994 there were no detection of GeV emission because no broad emission lines were observed. After 1995 May, however, the situation changed, broad optical emission lines emerged and so did GeV  $\gamma$ -rays. (Corbett et al. 2000).

Recently Böttcher et al. (2000) made a detailed study on the 1997 July  $\gamma$ -ray outburst in BL Lacertae and used an external Compton scattering model to explain the GeV  $\gamma$ -ray radiation with the seed photons coming from the broad line region, arguing that the broad optical line emission is in the right range of intensity and that the distance between the BLR and the burst source is such that there will be strong enough seed photons to produce the GeV emission. However, they emphasized that their model simply ignored the effects of the hard optical spectrum observed during this period.

Ravasio et al. (2002) suggested that for BL Lacertae, the IR–soft X-ray emission directly originates from synchrotron radiation, the hard X-ray – MeV emission is mainly due to synchrotron self-Compton process and the GeV emission is due to external Compton on the broad line photons by the same synchrotron electrons. In this case since the soft X-rays are due to the high-energy ‘tail’ of the electron distribution, the cooling time should be very short, while the hard X-rays produced via SSC by the lower energy electrons, should have much longer timescales. The observed timescales in soft X-rays and hard X-rays are consistent with these considerations. This kind of models have one electron population plus two sources for the seed photons.

All these studies on the  $\gamma$ -ray emission mechanism are closely related to the recent detections of broad emission lines in the source. However, in all these model-fittings to the SED of the 1997 July  $\gamma$ -ray flare, the authors adopted a very steep optical spectrum with  $\alpha_{\text{opt}}$  in the range of 1.1–1.6 (e.g. Böttcher et al. 2002), corresponding to assuming the synchrotron peak frequency to be quite low (e.g. Madejski et al. 1999).

Noticeably Tanihata et al. (2000) showed that during the 1997 July  $\gamma$ -ray flare the soft

X-ray spectrum is very steep ( $\alpha_x \sim 3-4$ ) and the spectral cutoff is located at  $\sim 100\text{eV}$ . This contrasts with the value of  $\sim 1\text{eV}$  adopted by Madejski et al. (1999). Therefore we can see that in the previous studies of the  $\gamma$ -ray emission mechanism for BL Lacertae two observational facts have been ignored : (1) the hard optical spectrum observed by Webb et al. (1998) and (2) the steep spectrum at soft X-ray waveband (or spectral cutoff at EUV wavelengths, see below). In other words the studies all assumed that the spectral cutoff of the synchrotron component occurs in the optical for the 1997 July  $\gamma$ -ray flare. Previously, Mukherjee et al. (1997) had pointed out that the Böttcher – Collmar model (1998) for the  $\gamma$ -ray emission observed in the low-polarization quasar PKS 0528+134 (Mukherjee et al. 1999) generally had problems when ignoring the observed hard optical spectra.

In this paper, we will re-investigate the SEDs of the  $\gamma$ -ray flare and demonstrate that the combination of the above facts implies that the synchrotron peak is in the EUV-soft X-ray bands ( $\sim 2 \times 10^{16}$  Hz) and hence SSC mechanism may possibly be important in the production of the GeV  $\gamma$ -ray emission. In the following we first recapitulate the observational properties in the optical, X-ray and  $\gamma$ -ray bands of the 1997 July GeV  $\gamma$ -ray flare, and then give the model-fitting results in terms of an SSC model.

## 2 RECAPITULATION OF THE PROPERTIES OF THE 1997 JULY FLARE

In this section we will recapitulate the main properties of the GeV  $\gamma$ -ray flare, for which a multi-frequency monitoring campaign was carried out in the optical, X-ray and MeV–GeV bands. The  $\gamma$  emission ( $>100\text{MeV}$ ) was observed by EGRET on board CGRO, the X-ray emission by ASCA and RTXE, and the optical emission by ground multi-color observations (Bloom et al. 1997; Tanihata et al. 2000; Webb et al. 1998). This outburst is particularly valuable for investigating correlations between different wavelengths and the mechanisms for the  $\gamma$ -ray emission.

### 2.1 Hard Optical Spectra

Bloom et al. (1997) made detailed observations of the optical flare in the  $R$ -band. However, their observations did not cover the peaking period of the  $\gamma$ -ray flare itself (July 18.75–19.08 UT) and suggested presumably that the peak of the optical flare lagged behind the  $\gamma$ -ray flare by several hours. During the peaking period of the  $\gamma$ -ray flare, the observed maximum brightness of BL Lacertae is  $\sim 12.6^{\text{m}}$ , which is brighter than the magnitude ( $\sim 13.8^{\text{m}}$ ) at the beginning (at epoch  $\sim 18.7\text{UT}$ ) of the flare by about 1.2 mag. The optical flare lasted much longer than the  $\gamma$ -ray flare.

Webb et al. (1998) carried out a multi-color ( $I, R, B, V$ ) observations of BL Lacertae during the period June 27.5– July 22.5. From this broadband observation the variations in the spectral slope (or spectral index  $\alpha$ , defined as  $S_\nu \propto \nu^{-\alpha}$ ) are derived. In the analysis of the optical data they corrected for the interstellar reddening, using  $E(B - V) = 0.36$  mag and  $A_V = 1.2$  mag. They also corrected for the underlying galaxy, using the derived flux densities of the host galaxy of BL Lacertae given by Brown et al. (1989). Their results can be summarized as follows.

- (1) The spectral variations show that the optical spectrum apparently flattens as the brightness of the source increases; the optical spectrum is hard and shows a large amount of variability in spectral index over the range 0.26–0.79 (15 spectra); the amplitude of variability is observed to be larger toward the blue end of the spectrum than the red.

- (2) Especially, on July 19.2 UT (JD 2450648.7) which is the only epoch of the optical observations nearest to the gamma-ray flaring period (July 18.75–19.08 UT), an optical peak was observed by Webb et al. (1998) at ( $B, V, R, I$ ) wavelengths. This peak has the highest brightness with R-magnitude 12.62<sup>m</sup>, agreeing precisely with the measurement by Bloom et al. (1997). The corresponding  $R$ -band flux density is  $\sim 52$  mJy and spectral index is  $\alpha \simeq 0.37 \pm 0.09$  which is one of the three flattest spectra observed during the optical monitoring period.

It can be seen that the optical observations made by Webb et al. (1998) clearly show that the optical spectrum observed during the  $\gamma$ -ray flaring period is much flatter than was observed previously (e.g., Smith et al. (1986); Brown et al. (1989); Bregman et al. (1990); Kawai et al. (1991); Sambruna et al. (1999); Madejski et al. (1999); Webb et al. (1998); Böttcher & Bloom (2000); Padovani et al. (2001); Ravasio et al. (2002)). For example, Brown et al. (1989) have observed that the optical spectral index of BL Lacertae varied in the range from 1.6 to 2.2 with a median of 2.0 (four spectra). The multicolor ( $IRVB$ ) data (obtained by Smith (1986)) re-analyzed by Webb et al. give a resulting spectral index varying in the range 0.79–1.64 with an average of 1.21 (17 spectra).

We suggest that the ‘multipeak’ morphology, characterizing many BL Lac optical flares observed in BL Lacertae, makes it difficult to associate particular optical peaks with particular gamma-ray peaks. However, the flatness of the optical spectra observed during the  $\gamma$ -ray flare period may be a real important feature. Since in their data reduction Webb et al. have taken out the non-variable host galaxy component, and since polarization measurements rule out the possibility that the spectral variability is due to a strong thermal accretion disk component (Smith 1986), the flattening of the spectrum observed during the  $\gamma$ -ray flare period is certainly related with the synchrotron emitting source component. There are three possible physical explanations for the spectral variability (wavelength-dependent variability): (a) the electron energy distribution for the synchrotron emission changes its slope, becoming flatter when the source brightens; (b) the turnover frequency is variable and is located in the optical; (c) there is more than one variable synchrotron component, each contributing to the optical continuum and each varying separately. In the following we will argue that the X-ray observations made by Tanihata et al. (2000) favors the first explanation.

Comparing the results given by Webb et al. (1998) and by Bloom et al. (1997), we found that the  $R$ -band magnitudes given by them are mutually consistent within  $\sim 0.1$  mag. During the  $\gamma$ -ray flaring period (July 18.75–19.8 UT), the R-magnitude measured by Bloom et al. is in the range 12.5<sup>m</sup>–12.9<sup>m</sup>, corresponding to flux density range 57.5–39.8 mJy.<sup>1</sup> Because of lack of optical sampling during the  $\gamma$ -ray peaking period and because of possible optical lag, it is impossible to choose an accurate optical flux to match the  $\gamma$ -ray peak (this is also not necessary, see below). In the following we will choose the  $R$ -band ( $4.3 \times 10^{14}$  Hz) flux density to be 50 mJy and the spectral index to be 0.40 (for the wavebands  $I, R, V,$  and  $B$ ).

As already mentioned above, during the period from 1982 to 1999 several authors studied the observed optical spectral properties of BL Lacertae, using a similar extinction law to correct for the reddening by the interstellar dust:  $E(B - V) = 0.36 - 0.39$  mag and  $R_V = 3.1 - 3.2$  (e.g., Brown et al. 1989; Webb et al. 1998; Sambruna et al. 1999; Ravasio et al. 2002). They gave spectral index at optical wavelengths in the range of 0.8–2.2. However during the  $\gamma$ -ray outburst in 1997, the optical spectrum dramatically flattens. The flattening of the optical spectrum during  $\gamma$ -ray outbursts are observed in other  $\gamma$ -ray blazars. For example, hard optical

<sup>1</sup> Here we use the transformation from R-magnitude to flux density:  $F_R = 10^{-0.4m_R+6.760}$ .

spectra have been detected in PKS0528+134. Mukherjee et al. (1997, 1999) pointed out that, for PKS 0528+134, in some observing periods, the optical spectrum shows an upturn compared to the overall synchrotron spectrum. They argued that this upturn is clearly not related to a ‘big blue bump’ due to direct accretion disk radiation, which in the case of PKS0528+134 would imply an accretion disk luminosity of approximately  $10^{48}$  erg s $^{-1}$ . Qian et al. (1998a, 1998b) has pointed out that, the 1994 TeV flare detected in Mrk 421 (Buckley et al. 1996; Macomb et al. 1995; Takahashi et al. 1996) may be associated with a synchrotron flare with a flat spectrum in the optical — X-ray band ( $\alpha_{\text{opt}} \sim 0.25$ ). The component caused the synchrotron peak to shift to  $\gtrsim 10$  keV, producing a large X-ray flare, but at optical wavelengths the flux density only shows a small change. This observational fact clearly indicates that there is another component that dominates the optical emission. A similar case has been observed for the TeV blazar Mrk 501 (a HBL). In Mrk 501, during the high energy flare of 1997 April 16, the synchrotron peak shifted to  $\gtrsim 100$  keV and the spectrum at 1 keV is very flat (spectral index  $\alpha_{1 \text{ keV}} \simeq 0.4$ ). Correspondingly, the GeV — TeV spectrum also becomes flatter. This TeV  $\gamma$ -ray flare can be interpreted in terms of the SSC mechanism, which shows that the source component has a flat electron energy distribution, and so with minor variations in the optical bands (Qian et al. 1998a, 1998b; Pian et al. 1998; Kataoka et al. 1999). That is, the optical emission is not dominated by the  $\gamma$ -ray emitting component but is produced by another component (presumably) with a steeper electron energy distribution. The fact that minor variations in the optical are associated with large amplitude variations in the X-ray —  $\gamma$ -ray bands, may imply that  $\gamma$ -ray outbursts are associated with the emergence of a flat energy distribution of relativistic electrons.

Thus from the above analysis we come to the conclusion that the hard optical spectra observed during the  $\gamma$ -ray outburst of BL Lacertae may provide evidence for the emergence of a flaring component with a flat energy distribution of relativistic electrons and for effective mechanisms of electron acceleration (Chiaberge & Ghisellini 1999; Romanova & Lovelace 1997). In the next Section we will show that the soft X-ray observations are consistent with this conclusion.

## 2.2 Steep Soft X-ray Spectrum

Within the period 1997 July 18.60–19.62 UT, BL Lacertae was also observed with ASCA ( $\sim 0.7 - 10$  keV) and also with RXTE ( $\sim 0.1 - 20$  keV) during two short intervals, July 18.78–18.80 UT and 19.30–19.32 UT (Tanihata et al. 2000). The observations showed a very high state of X-ray emission with its flux density in 2–10 keV band peaking at  $\sim 3.3 \times 10^{-11}$  erg cm $^{-2}$ s $^{-1}$ . This value is more than 3 times higher than that measured by ASCA in 1995 January when its GeV emission was first detected by EGRET. A detailed analysis of the spectral properties of these X-ray observations was performed by Tanihata et al. (2000). Two rapid flares were detected, but only in the soft X-ray band (0.7–1.5 keV), one of which peaked at  $\sim 19.0$  UT, coinciding with the  $\gamma$ -ray flare (18.75–19.08 UT). In the hard X-ray band (3–7 keV) the flux variations show a much longer time scale. The most interesting result is that the X-ray spectrum of the source during the observing period (18.60–19.62 UT) could be well fitted only by a two power-law model (plus Galactic absorption), i.e., the X-ray spectrum consists of two power-law components with the low-energy component dominating below  $\sim 1$  keV. In order to study the spectral variations in the X-ray band, the entire ASCA observation was divided into nine time intervals, for each of which the spectral index and integrated flux density were determined, using double power law fits for (0.7–1.5 keV) band and (3–7 keV) band, respectively. Tanihata et al. (2000) found that the soft X-ray power-law dominates the lower energy X-ray emission

during the flaring states, and the lower-energy spectrum is very steep with a radiation spectral index  $\alpha_x$  of 2–4. It appears to vary significantly during the period of observation. However, the hard power-law has a spectral index between  $\sim 0.3$  and  $0.6$ , and varies a little. It can be seen from table 3 of Tanihata et al. (2000) that for the time interval 4 when the  $\gamma$ -ray emission was detected and the soft X-ray flare peaked, the soft X-ray spectral index  $\alpha_x$  (0.7–1.5 keV) is  $3.7 \pm 0.5$ . This is the steepest index for the ASCA observing period. Correspondingly, the X-ray flux density in the (0.7–1.5 keV) band is  $(8.9 \pm 0.7) \times 10^{-12}$  erg cm $^{-2}$  s $^{-1}$ , which is also the highest flux density during the observing period.

The amplitude of flux variation is different for the two power-laws. For the hard component it is about a factor of 2, but for the soft component it is about a factor of 4. Thus it is clear that, the steepest and the strongest soft X-ray component emerged very closely to the  $\gamma$ -ray outburst, and the soft X-ray and the  $\gamma$ -ray flares may be produced by the same energy distribution of relativistic electrons in the same emitting region. From the values given above for the integrated flux density and spectral index for the time interval 4, we derived that at the peaking of the  $\gamma$ -ray flare the flux density of the soft component is  $F(1 \text{ keV}) \simeq 4.4 \mu\text{Jy}$ . In the following discussions we will adopt this value of flux density and a spectral index of 3.7(0.7–1.5 keV) to construct the synchrotron SED in combination with the optical data.

In addition, from the different properties of the soft and hard X-ray components (spectral index and variability time scale) it is clear that the soft and hard X-ray components are produced by different mechanisms: soft X-ray component is due to synchrotron radiation and the hard X-ray component due to SSC radiation (Makino et al. 1999).

Finally, we point out that the X-ray data collected by Giommi et al. (2002) for BL Lacertae have clearly confirmed the existence of a steep-spectrum soft X-ray component in some cases.

### 2.3 Gamma-ray Emission

BL Lacertae was monitored by the EGRET on board the Compton Gamma Ray Observatory in the period of 1997 July 15–22 (Bloom et al. 1997). A dramatic increase in the  $\gamma$ -ray flux by a factor of  $\sim 2.5$  was detected during the period of July 18.75–19.08 UT, when the average flux density ( $> 100$  MeV) was  $1.71 \times 10^{-6}$  photons cm $^{-2}$  s $^{-1}$ , more than 4 times the highest level previously observed in 1995 January (Catanese et al. 1997). The flux decreased to its previous level within  $\sim 8$  h. The  $\gamma$ -ray emission of the flare can be well fitted by a single power law with a spectral index  $\alpha_\gamma$  (100 MeV–10 GeV)  $\simeq 0.68$ . In comparison, the  $\gamma$ -ray spectrum observed in 1995 January has a spectral index of 1.27. Thus the spectrum during the 1997 outburst is significantly harder than the previous detection at a lower state. This behavior (i.e.,  $\gamma$ -ray spectrum hardens when the source brightens) is consistent with the usual behaviour of  $\gamma$ -ray blazars (e.g., Sambruna et al. 1999; Mukherjee et al. 1997, 1999), and is probably caused by the fresh acceleration (or injection) of higher energy electrons. Interestingly, we note that the spectral flattening in the  $\gamma$ -ray band is paralleled in the optical band, which may imply the synchrotron peak frequency shifting to UV–EUV bands and the synchrotron optical–UV photons playing an important role in the production of the  $\gamma$ -ray emission.

Since the peak of the gamma-ray flare cannot be precisely determined and the sampling of the coordinated optical data does not completely cover the period of the  $\gamma$ -ray flare, it is difficult to conclude with certainty as to whether the  $\gamma$ -ray flare precedes or lags behind the optical flare. However, Bloom et al. (1997) suggested that the  $\gamma$ -ray flare precedes the optical flare by a few hours. In some blazars different time sequences have been recorded. For example, the 1991 June  $\gamma$ -ray flare of 3C 279 showed the  $\gamma$ -ray peak lagging behind the optical peak by  $\sim 1$  day

(Hartman et al. 1996). Similar effect was observed in PKS 1406–076 (Wagner et al. 1995). To interpret the case of optical emission lagging behind the  $\gamma$ -ray emission in the framework of SSC scenario, the optical flare might be due to more than one emitting regions: a region emitting high-energy radiation provides the seed photons for the  $\gamma$ -ray flare while other regions produce the optical peak.

Comparing the light curve of the soft X-rays (0.7–1.5 keV) observed with ASCA (Makino et al. 1999; Tanihata et al. 2000) with the  $\gamma$ -ray light curve, we found that the soft X-ray flare peaking at July 18.9–19.0 UT is precisely simultaneous with the peaking of the  $\gamma$ -ray flare. Because the soft X-ray flare (with a timescale of  $\sim 5$  hours) indicates the occurrence of the high energy ‘tail’ of the synchrotron radiation, the simultaneity of the peaks points to the significance of synchrotron emission as the source of seed photons.

### 3 SED OF SYNCHROTRON COMPONENT

In order to investigate the mechanism of the production of  $\gamma$ -ray emission from blazars, it is crucial to study the SED of the synchrotron component and the correlation between the variability in the optical — X-ray and  $\gamma$ -ray bands

From the observations in the optical and soft X-ray bands described in the last section, we can derive the synchrotron spectrum of the 1997 July  $\gamma$ -ray flare. It is found that the observed flux densities and the spectral indices observed in optical and X-ray bands (Webb et al. 1998; Tanihata et al. 2000) can be well fitted with a synchrotron spectrum emitted by a power law energy distribution of relativistic electrons with a high-energy cutoff in a random magnetic field (Pacholczyk 1970, 1977).

In Fig. 1 is shown the fit to the observed flux densities and spectral indices in the optical and soft X-ray (0.75–1.5 keV) bands, using the results given by Pacholczyk (1977). The adopted power law energy index of the distribution and the cutoff frequency are 1.75 and  $4.3 \times 10^{16}$  Hz, respectively. It can be seen that the peak of the synchrotron SED (in the  $\nu F_\nu$  diagram of Fig. 1b) is located at  $\sim 2 \times 10^{16}$  Hz ( $\sim 100$  eV). In the study of the mechanism of the  $\gamma$ -ray emission of BL Lacertae, Madejski et al. (1999) placed the synchrotron peak at about 1 eV ( $2.4 \times 10^{14}$  Hz). This low peak energy led to the conclusion that, in the SSC scenario, an extremely large Lorentz factor of bulk motion ( $\sim 100$ ) and a very weak magnetic field strength ( $\sim 10^{-4}$  G) were required. These values are not acceptable and the SSC mechanism for the  $\gamma$ -ray emission was rejected. However, the analysis given above indicates that this synchrotron peak energy is much higher than that adopted by Madejski et al. (1999) and others (e.g. Sambruna et al. 1999) by a factor of  $\sim 100$ , implying that the contribution from the SSC process may be much more significant than in those models. In fact, using the synchrotron peak energy of  $\sim 100$  eV and the values for the other parameters given by Madejski et al., the bulk Lorentz factor and the magnetic field strength can be re-estimated in the SSC mechanism. It can be easily confirmed that they are now in the acceptable range. Thus we come to the conclusion that the SSC mechanism may be appropriate to explain the  $\gamma$ -ray emission observed in BL Lacertae (or at least SSC makes a significant contribution to the observed GeV  $\gamma$ -ray emission). As Qian et al. (1998a, b) have proposed, for  $\gamma$ -ray flares observed in BL Lacertae objects acceleration of flat energy distribution of relativistic electrons may be a common phenomenon, like in Mrk 421 and Mrk 501, such a flat energy distribution can extend to very high energies (10–100 keV) causing even TeV  $\gamma$ -ray emission, but they cannot contribute significantly in the optical bands (Pian et al. 1998; Macomb et al. 1995).

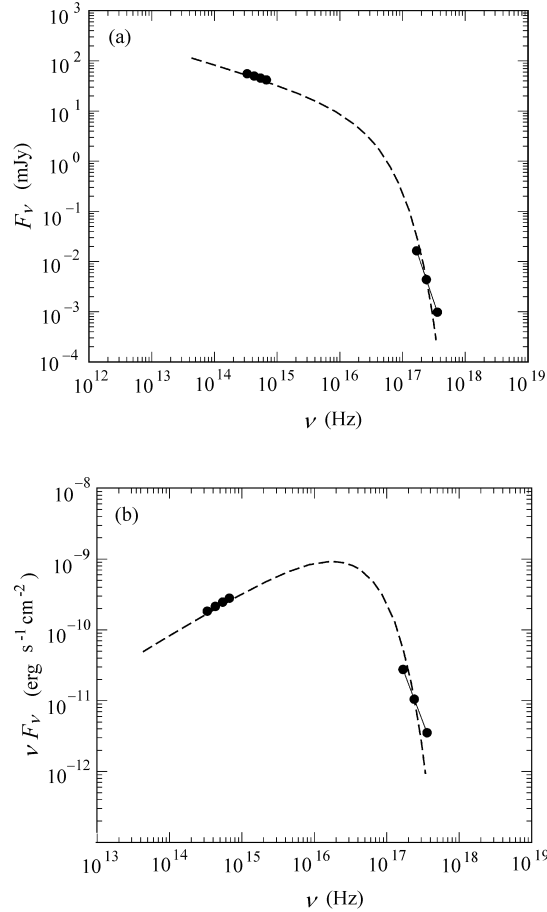


Fig. 1 (a) Observed optical and soft X-ray flux densities and spectral indices fitted with the synchrotron spectrum of a power-law energy distribution of relativistic electrons with a high energy cutoff. The adopted power law energy index of the distribution is 1.75 and the cutoff frequency is  $4.3 \times 10^{16}$  Hz; (b) The corresponding SED of the synchrotron emission in the  $\nu - \nu F_\nu$  diagram.

## 4 SYNCHROTRON SELF-COMPTON MODEL

### 4.1 Introduction

As we argued above, both the optical (Webb et al. 1998) and X-ray (Tanihata et al. 2000) observations simultaneous with the GeV  $\gamma$ -ray observation indicate that the peak of the synchrotron component is located in the EUV band. Thus the GeV  $\gamma$ -ray emission may be significantly due to SSC radiation mechanism. However, as Makino (1999) pointed out, the multi-frequency spectrum of this flare observed in BL Lacertae cannot be interpreted by a single component SSC model. So we have tried to seek for a two-component model to interpret the entire high-energy emission from hard X-rays to GeV  $\gamma$ -rays.

Very recently, an internal shock scenario has been proposed for interpreting the  $\gamma$ -ray emissions from blazars (Spada et al. 2001). In this scenario two emitting regions are formed in a two-shell collision in the jet: one is related to the forward shock and the other, to the reverse shock. The latter region thus may be identified as the GeV emitter and the former as the lower-energy one, since the latter is associated with the fast shell with a larger bulk Lorentz factor, presumably implying acceleration of more energetic electrons. As a qualitative scheme, this is adequate for our case, but more theoretical studies are required to investigate the relationship between the physical parameters in the two-shell collision and this is beyond the scope of this paper (see Spada et al. 2001). In the following we only make a model-fit to the observed SED in terms of a two-component model.

#### 4.2 Estimation of Model Parameters

Synchrotron self-Compton models have been widely applied to explain  $\gamma$ -rays from blazars, mostly those in HBLs. In general, SSC models involve a number of parameters which cannot be determined from the model-fit of a single SED. However, in SSC models the physical parameters of the emitting region can be estimated from the measured quantities (For example, Kubo et al. 1998; Tavecchio et al. 1998). This will help in the choice of the parameters. We assume that the emitting region is homogeneous, in the form of a sphere with a radius  $R$  and that the energy distribution of the relativistic electrons is described by a single broken power-law with a break  $\gamma_b$ . In this case some relations for the physical parameters of the emitting region can be given as follows.

— It is usually assumed that  $R \lesssim c\Delta t \frac{\delta}{1+z}$ , where  $\Delta t$  is the observed variability timescale and  $\delta$  is the Doppler factor.

— The peak frequency of the synchrotron component in the observer frame is,

$$\nu_s(\text{Hz}) = 1.2 \times 10^6 \gamma_b^2 B \frac{\delta}{1+z}. \quad (1)$$

Here  $\gamma_b$  is the energy break of the energy distribution of the relativistic electrons and  $B$  is the magnetic field in Gauss.

— In the Thomson regime the expected peak of the SSC component in the observer frame is given by

$$\nu_c = \frac{4}{3} \gamma_b^2 \nu_s. \quad (2)$$

— The ratio of the observed luminosity of the SSC component  $L_c$  to the synchrotron component luminosity  $L_s$  is

$$\frac{L_c}{L_s} = \frac{U_s}{U_B}, \quad (3)$$

where  $U_s$  is the energy density of the synchrotron radiation in the comoving frame,  $U_s = L_s / (4\pi R^2 c \delta^4)$ .  $U_B = B^2 / 8\pi$  is the magnetic field energy density.

— From the equations given above we derive

$$\delta^4 \gtrsim 1.6 \times 10^{12} \frac{L_s^2}{c^3 \Delta t^2 L_c} \frac{\nu_s^2}{\nu_c^4}. \quad (4)$$

— We have the equation for  $B$

$$B = 2.7 \times 10^{-20} (R_{\text{pc}} \delta^2)^{-1} \sqrt{\frac{L_s^2}{L_c}}, \quad (5)$$

where  $R_{\text{pc}}$  is the radius in units of parsec.

— We have the energy break,

$$\gamma_b = 1.8 \times 10^3 (R_{\text{pc}} \delta)^{\frac{1}{2}} [\nu_s (1+z)]^{\frac{1}{2}} \left[ \frac{L_s^2}{L_c} \right]^{-\frac{1}{4}}. \quad (6)$$

From the observed SED and variability timescale for the flare we obtain values of the observables:  $\Delta t < 8$  h,  $\nu_s \sim 2 \times 10^{16}$  Hz,  $\nu_c \sim 30$  GeV,  $L_s \sim 8.5 \times 10^{45}$  erg s $^{-1}$  and  $L_c \sim 4.7 \times 10^{45}$  erg s $^{-1}$ . From these values we derive  $R < 8.6 \times 10^{15}$  cm,  $\delta \gtrsim 4.4$ ,  $B \sim 2$  G and  $\gamma_b \sim 10^4$ .

Besides these values we will need the values of the normalization factor  $K_1$  of the energy distribution of the relativistic electrons and the energy indices  $\alpha_1$  and  $\alpha_2$ . From the analysis we have  $\alpha_1 \sim 0.3 - 0.4$  and  $\alpha_2 \sim 4 - 4.5$ .  $K_1$  can be obtained from the self-absorption turn-over of the synchrotron spectrum.

Having estimated the physical parameters for the GeV emitting region we point out that the relatively narrow band of the synchrotron component in frequency range implies that the emission from hard X-ray to MeV energies could be due to another emitting region. We can also estimate its physical parameters with the procedure similar to that described above, although it is less constrained, because of lack of submm — IR data. However, the parameters for the second component are constrained by the hard X-ray observations.

### 4.3 An Assumption on the Electron Energy Distribution

From the discussion in Sect. 3 we have seen that the synchrotron spectrum can not be well described by a single broken power law, because of its steep continuous curvature around the cutoff frequency. Thus as in general, on the basis of the phenomenological shape of the observed synchrotron spectrum, we would assume that the energy distribution of the relativistic electrons has a continuously curved shape (Fossati et al. 1998).

$$N(\gamma) = K \gamma^{-n_1} \left( 1 + \left( \frac{\gamma}{\gamma_b} \right)^f \right)^{(n_1 - n_2)/f}, \quad (7)$$

where  $\gamma_b$  is the break energy and,  $n_1$  and  $n_2$  are the energy indices at lower and higher energies;  $n_1 = 2\alpha_1 + 1$ ,  $n_2 = 2\alpha_2 + 1$ . In our case  $\alpha_1 \simeq 0.3 - 0.4$ , and  $\alpha_2 \simeq 4.0 - 4.5$ ;  $f$  is a parameter which determines the specific shape of the curvature.

However, for this expression of the electron energy distribution the calculation of both synchrotron and Compton radiation is quite complicated. In order to simplify the calculation, we would use a few power-laws to approximate the distribution, whereby the Compton emission can be calculated by using the  $\delta$ -function approximation for each pair of power-laws for the electrons and photons (see below, and Tavecchio et al. 1998; Königl 1981).

### 4.4 $\delta$ -function Approximation

In the following we will apply the synchrotron self-Compton mechanism to interpret the SED of the 1997 July  $\gamma$ -ray flare of BL Lacertae. We will not include the radio emission because it is thought to be produced in a much larger emitting region which is not associated with the high energy emitting region in the optical, X-ray and  $\gamma$ -ray bands.

We consider a population of relativistic electrons, which is described by three power-laws with two energy breaks ( $\gamma_{e, b1}$ ,  $\gamma_{e, b2}$ ) and a high energy cutoff ( $\gamma_{e, \text{cut}}$ ), i.e., the energy distribution of the relativistic electrons is divided into three branches:

$$\text{For } \gamma_{e, \text{min}} \leq \gamma_e \leq \gamma_{e, b1} \quad N(\gamma_e) = K_{e1} \gamma_e^{-(2\alpha_{e1}-1)}. \quad (8)$$

$$\text{For } \gamma_{e,b1} \leq \gamma_e \leq \gamma_{e,b2} \quad N(\gamma_e) = K_{e2} \gamma_e^{-(2\alpha_{e2}-1)}. \quad (9)$$

$$\text{For } \gamma_{e,b2} \leq \gamma_e \leq \gamma_{e,\text{cut}} \quad N(\gamma_e) = K_{e3} \gamma_e^{-(2\alpha_{e3}-1)}. \quad (10)$$

$$\text{For } \gamma_e > \gamma_{e,\text{cut}} \quad N(\gamma_e) = 0. \quad (11)$$

Here  $N(\gamma_e)$  is the differential electron density,  $\gamma_e$  is the Lorentz factor of a relativistic electron. Correspondingly, the synchrotron emissivity  $\epsilon_s(\nu_s)$  can be described by a set of four power-laws, i.e., the synchrotron emission is divided into four branches:

$$\text{For } \nu_{t,\text{min}} \leq \nu_s \leq \nu_{s,b1} \quad \epsilon_s(\nu_s) = \epsilon_s(\nu_{t,\text{min}}) \left( \frac{\nu_s}{\nu_{t,\text{min}}} \right)^{-\alpha_{s1}}. \quad (12)$$

$$\text{For } \nu_{s,b1} \leq \nu_s \leq \nu_{s,b2} \quad \epsilon_s(\nu_s) = \epsilon_s(\nu_{s,b1}) \left( \frac{\nu_s}{\nu_{s,b1}} \right)^{-\alpha_{s2}}. \quad (13)$$

$$\text{For } \nu_{s,b2} \leq \nu_s \leq \nu_{s,\text{cut}} \quad \epsilon_s(\nu_s) = \epsilon_s(\nu_{s,b2}) \left( \frac{\nu_s}{\nu_{s,b2}} \right)^{-\alpha_{s3}}. \quad (14)$$

$$\text{For } \nu_s > \nu_{s,\text{cut}} \quad \epsilon_s(\nu_s) = \epsilon_s(\nu_{s,\text{cut}}) \left( \frac{\nu_s}{\nu_{s,\text{cut}}} \right)^{-\alpha_{s4}}. \quad (15)$$

Here  $\alpha_{s1}$ ,  $\alpha_{s2}$  and  $\alpha_{s3}$  are equal to  $\alpha_{e1}$ ,  $\alpha_{e2}$  and  $\alpha_{e3}$ , respectively;  $\alpha_{s4}$  describes the spectrum beyond the cutoff frequency and we assume  $\alpha_{s4} = 4.0$  or  $4.5$ ;  $\nu_{t,\text{min}}$  is the low frequency turnover, below which the spectrum is described by a power law with an index of  $-2.5$ ;  $\nu_{s,b1}$ ,  $\nu_{s,b2}$  and  $\nu_{s,\text{cut}}$  are the emitting frequencies corresponding to the electron energies  $\gamma_{b1}$ ,  $\gamma_{b2}$  and  $\gamma_{\text{cut}}$ , respectively.

Following Königl (1981) and using the  $\delta$ -function approximation (e.g., Rieke & Weekes 1969), the emissivity  $\epsilon_c(\nu_c)$  of inverse-Compton radiation due to a single scattering of synchrotron photons (with a spectral index  $\alpha_s$ ) by relativistic electrons (with a energy spectral index  $\alpha_e$ ) can be calculated. According this approximation, the final frequency of a scattered photon is given by  $\nu_c \approx \gamma_e^2 \nu_s$  for the Thomson regime ( $\gamma_e h \nu_s \leq m_e c^2$ ). For the Klein-Nishina regime ( $\gamma_e h \nu_s \geq m_e c^2$ )  $\nu_c \approx \gamma_e m_e c^2 / h$ . Here  $\nu_s$  is the initial frequency of the photon,  $\gamma_e$  is the Lorentz factor of the scattering electron,  $m_e$  is the electron's rest mass and  $h$  is the Planck constant.

We will calculate the synchrotron self-Compton radiation first for each pair of power law distributions of photons and electrons, and then sum up the results for all the pairs (similar calculations were performed by Tavecchio et al. (1998)). Following Königl (1981) the inverse-Compton emissivity  $\epsilon_c(\nu_c)$  is calculated by using the approximate formulae for Thomson scattering regime and Klein-Nishina regime, respectively. For a specific pair of power law distributions of photons and electrons described by power-law indices of  $\alpha_s$  and  $\alpha_e$  (here we neglect the suffix 1-4), in the comoving frame we have the emissivity  $\epsilon_c^T$  due to Thomson scattering:

$$\epsilon_c^T(\nu_c) \approx K_e \sigma_T R \epsilon_s(\nu_c) \int_{\gamma_{\text{min}}}^{\gamma_{\text{max}}} \gamma^{2(\alpha_s - \alpha_e) - 1} d\gamma, \quad (16)$$

$$\gamma_{e,\text{min}}^2 \nu_{s,\text{min}} \leq \nu_c \leq \min[\gamma_{e,\text{max}}^2 \nu_{s,\text{max}}; \gamma_{e,\text{max}} m_e c^2 / h; (m_e c^2 / h)^2 / \nu_{s,\text{min}}], \quad (17)$$

where

$$\gamma_{\text{min}} = \max[\gamma_{e,\text{min}}; (\nu_c / \nu_{s,\text{max}})^{1/2}; h \nu_c / m_e c^2], \quad (18)$$

$$\gamma_{\text{max}} = \min[\gamma_{e,\text{max}}; (\nu_c / \nu_{s,\text{min}})^{1/2}]. \quad (19)$$

Here  $\sigma_T$  is the Thomson cross section,  $R$  is the radius of the emitting region, which is assumed to be a sphere;  $\alpha_s$ ,  $\alpha_e$ ,  $K_e$ ,  $\gamma_{e,\min}$ ,  $\gamma_{e,\max}$ ,  $\nu_{s,\min}$  and  $\nu_{s,\max}$  are parameters which correspond to the specific pair of the two power law branches describing the synchrotron radiation and the electron distribution.

The emissivity  $\epsilon_c^{\text{KN}}$  due to scattering in the Klein-Nishina regime is given by

$$\epsilon_c^{\text{KN}}(\nu_c) \approx f(\nu_c) \left[ \frac{\nu_c^{-(\alpha_s+1)}}{\alpha_s+1} \left\langle \frac{\alpha_s+3}{2(\alpha_s+1)} + \ln \left[ 2\nu_c \left( \frac{h}{m_e c^2} \right)^2 \right] \right\rangle \right]_{\nu_{\min}, \nu_{\max}}, \quad (20)$$

$$f(\nu_c) = \frac{3}{8} K_e \sigma_T R \epsilon_s(\nu_c) (m_e c^2 / h)^{2(\alpha_e+1)} \nu_c^{\alpha_s-2\alpha_e-1}, \quad (21)$$

$$\max[\gamma_{e,\min} m_e c^2 / h; (m_e c^2 / h)^2 / \nu_{s,\max}] \leq \nu_c \leq \gamma_{e,\max} m_e c^2 / h, \quad (22)$$

where  $\nu_{\min} = \max[\nu_{s,\min}; (m_e c^2 / h)^2 / \nu_c]$  and  $\nu_{\max} = \nu_{s,\max}$ . The total inverse-Compton emissivity  $\epsilon^c = \epsilon_c^T + \epsilon_c^{\text{KN}}$ .

#### 4.5 Specific Models

We have considered a SSC model to fit the SED of the 1997 July  $\gamma$ -ray outburst observed in BL Lacertae. It is shown that two emitting components are needed to reproduce the emission in the optical through  $\gamma$ -rays. Component-1 mainly produces the optical-soft X-ray radiation through synchrotron and the GeV emission through self-Compton scattering. The hard X-ray and MeV emission is produced from an associated component (component-2) through self-Compton scattering of sub-millimeter – infrared photons.

##### 4.5.1 Model-fit

This model is calculated for the observed optical spectral index of 0.40. As we have shown that the SED of the 1997 July flare can be fitted by a two-component SSC model, and the result is shown in Fig. 2. The values of the parameters are chosen following the estimations in the previous section.

We used a Doppler factor of 15.7, which is consistent with the values given in Sambruna et al. (1999), Ravasio et al. (2002) and Böttcher & Bloom (2000). We assumed that the Doppler factor of the component-2 is equal to that of the component-1, as is usually done in internal shock models (Spada et al. 2001). The values for the other parameters are as follows.

(1) Component-1 (GeV component):

$$\alpha_{s1}=0.3, \alpha_{s2}=0.8, \alpha_{s3}=1.3, \alpha_{s4}=4.5. \alpha_{ei}=\alpha_{si} \ (i=1-3). \gamma_{e,\min} = 1, \gamma_{e,b1} = 4.52 \times 10^3, \\ \gamma_{e,b2} = 1.04 \times 10^4, \gamma_{e,\text{cut}} = 3.20 \times 10^4, K_{e1} = 3.41 \times 10^3 \ (\text{cm}^{-3}), B = 1.04 \text{ G and } R = 4.06 \times 10^{15} \text{ cm.}$$

(2) Component-2 (MeV component):

$$\alpha_{s1}=0.52, \alpha_{s2}=0.52, \alpha_{s3}=1.02, \alpha_{s4}=4.0, \gamma_{e,\min}=1, \gamma_{e,b1} = 4.17 \times 10^2, \gamma_{e,b2} = 4.17 \times 10^3, \\ \gamma_{e,\text{cut}} = 6.42 \times 10^3, K_{e1}=1.09 \times 10^6 \text{ cm}^{-3}, B = 0.13 \text{ G and } R = 4.87 \times 10^{15} \text{ cm.}$$

We suggest that the values for the parameters of component-2 could be chosen over a much wider range. Stringent constraints on these can only be obtained through simultaneous observations in the IR – submillimeter band.

It can be seen from Fig. 2 that the proposed model can well fit the observed SED, especially the higher energy component (Compton component from hard X-ray to GeV). However, the lower energy synchrotron component remains to be confirmed by observations in the near future, because of the lack of available data, especially in the UV-EUV and IR-submm bands. In the SSC-model given above the high energy component-1 produces optical – UV – soft X-ray flare

and the GeV flare. Since the synchrotron radiation of this component has a flat spectrum in the IR–optical bands, its hard X-ray emission through SSC process is weak and cannot explain the observed hard X-ray emission. In our model the hard X-rays are due to a low energy component (component-2). Its synchrotron peak is located in the submillimeter–infrared bands ( $\lesssim 10^{14}$  Hz) with a steep spectral index in the optical band. The MeV emission is mainly produced by this component. Thus our model-fit suggests that the flaring region has a two-component structure which may be related to the double emitting regions of a relativistic shock in the jet.

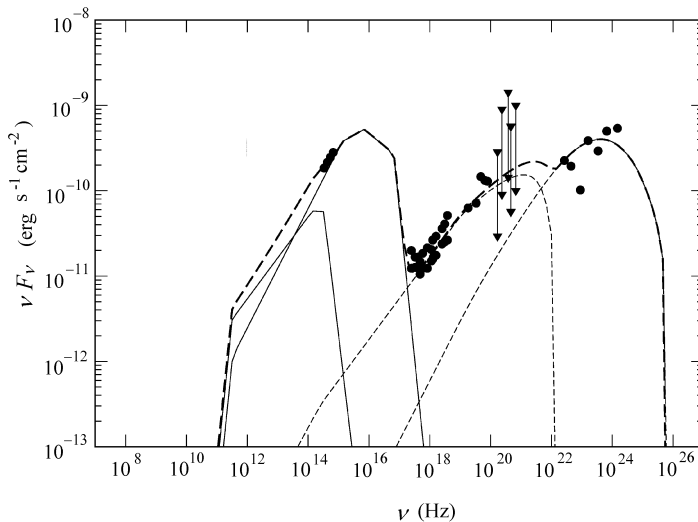


Fig. 2 A SSC model-fit to the SED of the  $\gamma$ -ray flare observed in 1997 July in BL Lacertae. The observed optical spectral index  $\alpha_{\text{opt}}$  is taken to be 0.40.

We show that the values of the parameters chosen for the model-fits satisfy the conditions required by the observed timescales and the transparency to the GeV  $\gamma$ -rays. For the size ( $4 \times 10^{15}$  cm) and Doppler factor ( $\delta = 15.7$ ) of component-1, the timescale is calculated to be  $\sim 2.2$  hours, which is consistent with that observed for  $\gamma$ -ray flares.

According to Mattox (1993) the opacity for the GeV  $\gamma$ -rays due to pair-production is:

$$\tau_{\gamma} = 1.31 \times 10^3 \left( \frac{1+z}{\delta} \right)^{4+2\alpha_x} (1+z - \sqrt{1+z})^2 h_{100}^{-2} T_5^{-1} \frac{F_{1\text{keV}}}{\mu\text{Jy}} \left( \frac{E_{\gamma}}{\text{GeV}} \right)^{\alpha_x}, \quad (23)$$

where  $h_{100}$  is the value of Hubble constant  $H_0$  in units of  $100 \text{ km s}^{-1} \text{ Mpc}^{-1}$ ,  $T_5$  is the timescale in units of  $10^5$  s,  $z$  is the redshift of BL Lacertae (0.069). Taking  $\delta = 15$ ,  $\alpha = 4.0$ ,  $F_{1\text{keV}} = 4 \mu\text{Jy}$ ,  $E_{\gamma} = 10 \text{ GeV}$ ,  $T_{\text{obs}} = 10^4$  s and  $T_5 = 0.1$ , we obtain  $\tau_{\gamma} (10 \text{ GeV}) \ll 1$ .

## 5 DISCUSSION AND CONCLUSIONS

In the above we combined the optical and X-ray observations made during the 1997 July  $\gamma$ -ray outburst and showed that the synchrotron peak could be at  $\sim 2 \times 10^{16}$  Hz, instead of  $\sim 2 \times 10^{14}$  Hz as adopted by Madejski et al. (1999) and others. This clearly implies that during the 1997 July  $\gamma$ -ray outburst the peak frequency shifted toward higher energy bands.

Such a phenomenon has been observed in BL Lacertae objects Mrk 421 and Mrk 501 (two well known ‘high-energy peaked’ blazars), in which the synchrotron peak shifted toward 10–100 keV with a flat spectrum at optical – UV wavelengths. On the basis of this analysis we come to the conclusion that the synchrotron photon density may be high enough to produce the GeV  $\gamma$ -ray outburst through self-Compton process, and that it is not necessary to invoke external photons from, e.g., the broad line emitting clouds, as in the external Compton models where the presence of broad emission lines (Vermeulen et al. 1995; Corbett et al. 2000) is regarded as the main factor for the production of GeV  $\gamma$ -rays. In our model, the hard X-ray and MeV  $\gamma$ -rays are mainly produced by a lower energy component which might have a high energy cutoff at optical wavelengths, because the GeV emitting component has a much flatter spectrum and thus makes less contribution to the IR and MeV emission. This component could have longer timescales than the GeV emitting component. Correlation between hard X-ray – MeV emission and submillimeter – IR emission is a signature of the presence of the second lower energy component.

However, we do not rule out the contribution from the external Compton scattering of seed photons from the broad line emitting clouds. What we emphasize is that in the case of BL Lacertae synchrotron self-Compton process may still play a significant role in the production of the GeV  $\gamma$ -ray emission. Simultaneous UV–EUV observations with satellites thus are important to distinguish between the two types of models. In our model variability in GeV and in UV–EUV bands should be correlated and the synchrotron peak should shift toward the EUV band during GeV  $\gamma$ -ray flares. Submillimeter–IR observations are also important to find the correlation between the variability in submillimeter–IR and in MeV emission with similar timescales (but not in GeV).

## References

- Bloom S. D., Bertsch D. L., Hartman R. C. et al., 1997, *ApJ*, 490, L145  
Böttcher M., Aller H. D., Aller M. F. et al., 2002, *astro-ph/0203379*  
Böttcher M., Bloom S. D., 2000, *AJ*, 119, 469  
Böttcher M., Collmar W., 1998, *A&A*, 329, L57  
Bregman J. N., Glassgold A. E., Huggins P. J. et al., 1990, *ApJ*, 352, 574  
Brown L. M. J., Robson E. I., Gear W. K. et al., 1989, *ApJ*, 340, 129  
Buckley J. H., Akerlof C. W., Biller S. et al., 1996, *ApJ*, 472, L9  
Catanese M., Akerlof C. W., Biller S. D. et al., 1997, *ApJ*, 480, 562  
Chiaberge M., Ghisellini G., 1999, *MNRAS*, 306, 551  
Corbett E. A., Robinson A., Axon D. J., Hough J. H., 2000, *MNRAS*, 311, 485  
Corbett E. A., Robinson A., Axon D. et al., 1996, *MNRAS*, 281, 737  
Fossati G., Maraschi L., Celotti A., Cosmatri A., Ghisellini G., 1998, *MNRAS*, 299, 433  
Ghisellini G., Celotti A., Fossati G., Maraschi L., Cosmatri A., 1998, *MNRAS*, 301, 451  
Giommi P., Capalbi M., Fiacchi M. et al., 2002, *Astro-ph/0209596*  
Hartman R. C., Webb J. R., Marscher A. P. et al., 1996, *ApJ*, 461, 698  
Königl A., 1981, *ApJ*, 243, 700  
Kataoka J., Mattox J. R., Quinn J., Kubo H., Makino F., Takahashi T., Inoue S., Chartman R. C., Madejski G. M., Sreekumar P., Wagner S. J., 1999, *ApJ*, 514, 138  
Kawai N., Matsuoka M., Bregman J. N. et al., 1991 *ApJ*, 382, 508  
Kubo H., Takahashi T., Madejski G., Tashiro M., Makino F., Inoue S., Takahara F., 1998, *ApJ*, 504, 693

- Macomb D. J., Akerlof C. W., Aller H. D. et al., 1995, *ApJ*, 449, L99
- Madejski G. M., Sikora M., Jaffe T., Blazejowski M., Jahoda K., Moderski R., 1999, *ApJ*, 521, 145
- Makino F., Tanihata C., Takahashi T., Kataoka J., Kubo H., Kawai N., Mattox J. R., 1999, In: L. O. Takalo, A. Sillanpää, eds., *ASP Conference series*, Vol. 159, BL Lac Phenomenon, p.176
- Mattox J. R., Bertsch D. L., Chiang J. et al., 1993, *ApJ*, 410, 609
- Miller J. S., French H. B., Hawley S. A., 1978, *ApJ*, 219, L85
- Mukherjee R., Bertsch D. L., Bloom S. D. et al., 1997, *ApJ*, 490, 116
- Mukherjee R., Böttcher M., Hartman R. C. et al., 1999, *ApJ*, 527, 132
- Pacholczyk A. G., *Radio Astrophysics*, Freeman, 1970
- Pacholczyk A. G., *Radio Galaxies*, Pergamon Press, 1977
- Padovani P., Costamante L., Giommi P. et al., 2001, *MNRAS*, 328, 931
- Peterson B., 1997, *An Introduction to Active Galactic Nuclei* Cambridge: Cambridge Univ. Press
- Pian E., Vacanti G., Tagliaferri G. et al., 1998, *ApJ*, 492, L17
- Qian S. J., Zhang X. Z., Witzel A., Krichbaum T. P., Britzen S., Kraus A., 1998a, In: *ASP Conference series*, Vol. 144, Radio Emission from Galactic and Extragalactic Compact Sources, p.93
- Qian S. J., Zhang X. Z., Witzel A., Krichbaum T. K., Britzen S., Kraus A., 1998b, *Acta Astrophysica Sinica*, 18, 17
- Ravasio M., Tagliaferri G., Ghisellini G. et al., 2002, *A&A*, 383, 763
- Rieke G. H., Weekes T. C., 1969, *ApJ*, 155, 429
- Romanova M. M., Lovelace R. V. E., 1997, *ApJ*, 475, 97
- Sambruna R., Maraschi L., Urry C. M., 1996, *ApJ*, 463, 444
- Sambruna R. M., Ghisellini G., Hooper E., Kollgaard R. I., Pesce J. E., Urry C. M., 1999, *ApJ*, 515, 140
- Smith P. S., 1986, Ph.D. thesis, Univ. New Mexico
- Spada M., Ghisellini G., Lazzati D., Celotti A., 2001, *MNRAS*, 325, 1559
- Takahashi T., Tashiro M., Madejski G. et al., 1996, *ApJ*, 470, L89
- Tanihata C., Takahashi T., Kataoka J. et al., 2000, *ApJ*, 543, 124
- Tavecchio F., Maraschi L., Ghisellini G., 1998, *ApJ*, 509, 608
- Vermeulen R. C., Ogale P. M., Tran H. D. et al., 1995, *ApJ*, 452, L5
- Wagner S. J., Mattox J. R., Hopp U. et al., 1995, *ApJ*, 454, L97
- Ulrich M.-H., Maraschi L., Urry C. M., 1997, *ARA&A*, 35, 445
- Webb J. R., Freedman I., Howard E. et al., 1998, *AJ*, 115, 2244